

Phase aberration compensation in digital holographic microscopy based on principal component analysis

Chao Zuo,^{1,2,*} Qian Chen,¹ Weijuan Qu,³ and Anand Asundi²

¹Jiangsu Key Laboratory of Spectral Imaging & Intelligence Sense, Nanjing University of Science and Technology, Nanjing, Jiangsu Province 210094, China

²Centre for Optical and Laser Engineering, School of Mechanical and Aerospace Engineering, Nanyang Technological University, Singapore 639798

³Centre for Applied Photonics and Laser Technology, Ngee Ann Polytechnic, 535 Clementi Road, Singapore 599489

*Corresponding author: surpasszuo@163.com

Received February 20, 2013; accepted April 18, 2013;
posted April 19, 2013 (Doc. ID 185583); published May 14, 2013

We present an effective, fast, and straightforward phase aberration compensation method in digital holographic microscopy based on principal component analysis. The proposed method decomposes the phase map into a set of values of uncorrelated variables called principal components, and then extracts the aberration terms from the first principal component obtained. It is effective, fully automatic, and does not require any prior knowledge of the object and the setup. The great performance and limited computational complexity make our approach a very attractive and promising technique for compensating phase aberration in digital holography under time-critical environments. © 2013 Optical Society of America

OCIS codes: (090.1995) Digital holography; (090.1000) Aberration compensation; (090.2880) Holographic interferometry; (120.5050) Phase measurement.

<http://dx.doi.org/10.1364/OL.38.001724>

Digital holographic microscopy (DHM) is a powerful tool which allows the digital recording and numerical reconstruction of the complex wavefront of the samples so that the amplitude and phase of the wave reflected by the sample or transmitted through it can be quantitatively retrieved with high accuracy and in near real time [1]. The object wave is generally a spherical wave due to the use of a microscope objective to enhance the spatial resolution. This will introduce a spherical phase curvature, which needs to be compensated for in order to accurately recover the phase information induced by the object [2].

A lot of work has been done in the recent years to compensate this curvature of the wavefront in DHM. They can be categorized into two groups: physical [3–5] and numerical [1,6–11]. The physical methods are generally achieved by introducing the same curvature in the reference wave using a same objective lens [3] or a position-adjustable lens [4]. However, a precise alignment of the optical elements are required, and a perfect wavefront curvature matching between the object and reference arms is difficult to realize in practice. The numerical methods remove the phase aberration during postprocessing of the digital hologram. Double exposure [10] can compensate the inherent wavefront curvature completely, but they need an additional hologram recording without the samples. Other methods use a phase mask in either the reconstruction plane or hologram plane [6,8,10], or use two-dimensional fitting methods with a standard spherical surface [9] or Zernike polynomials [11] directly in the reconstructed phase map. Compared with the reconstruction plane approaches, compensation in the hologram plane avoids the need of adapting the phase mask when the reconstruction distance is changed [5,8]. But it involves additional two-dimensional phase unwrapping and numerical reconstruction. The

techniques listed above present some disadvantages, such as manual operation, preknowledge of the setup or/and the specimen under test, making them difficult to be fully automated. More importantly, existing methods, even for the simplest two-dimensional least-squares surface fitting method [9], reside on the large computational requirements, which make them costly from a processing and computational point of view, precluding real-time monitoring.

In this work, we present a novel numerical phase aberration compensation method based on the principal component analysis (PCA). This study is based on but not limited to the experimental setup for a transmission DHM system with the Michelson interferometer configuration, described in detail in [4]. The intensity distribution of the recorded hologram can be written as [1]

$$I_H(x, y) = |O|^2 + |R|^2 + RO^* + R^*O, \quad (1)$$

$R(x, y)$ and $O(x, y)$ are the reference and object waves, respectively, $*$ denotes the complex conjugate. Due to a small angle between the reference and object waves, the virtual image term then can be extracted by filtering the hologram's two-dimensional Fourier spectrum

$$I_H^r(x, y) = R^*O = |R||O| \exp[i\varphi(x, y)]Q(x, y), \quad (2)$$

where the $\varphi(x, y)$ is the phase of the test object. $Q(x, y)$ is the phase aberration term that needs to be compensated, which can be generally represented by

$$Q(x, y) = \exp[i(k_x x + k_y y)] \exp[i(l_x x^2 + l_y y^2)], \quad (3)$$

where the factors k_x, k_y denote the linear phase difference between O and R due to the off-axis geometry.

The parameters l_x, l_y in Eq. (3) describe the relative divergence between the object and reference beam due to the mismatch in spherical phase curvature. Normally, the spherical phase factor is physically compensated and the tilt term corrected by spectrum centering [8]. The typical process for DHM demodulation and reconstruction are illustrated in Fig. 1. However, the phase curvature is difficult to be completely eliminated, which also makes the spectrum centering (and hence tilt compensation) difficult because in that case the spectrum no longer demonstrates a punctual central frequency [4,8].

A close inspection of Eq. (3) reveals that the ideal model for $Q(x, y)$ is in fact a rank one matrix. This allows the definition of two vectors $p(x) = \exp[i(k_x x + l_x x^2)]$ and $q(y) = \exp[i(k_y y + l_y y^2)]$ with the phase aberration matrix rewritten as $Q(x, y) = pq^H$, where $\{\bullet\}^H$ denotes the complex-conjugate transpose. In other words, the phase aberration matrix should only have one principal component, which describes the single best subspace in the least-squares sense. As for thin objects localized in small areas, we may assume that their phase $\varphi(x, y)$ is a small perturbation to the overall reconstructed phase distribution. Therefore, the one principal component approximation of $\exp[i\varphi(x, y)]Q(x, y)$ should also be established. The illuminating feature of this is the problem of phase compensation is recast as finding the first principal component of the exponential term of the filtered hologram. A straightforward approach to perform PCA or finding the dominant rank one subspace of Q is to use the singular value decomposition. The linear and quadratic coefficients in p and q can then be identified independently on the unwrapped phase components of left and right dominant singular vectors using least-squares fitting. Once the coefficients of $Q(x, y)$ have been determined, its conjugate $Q^H(x, y)$ can be multiplied with the filtered hologram, leading to an aberration-free virtual image term:

$$Q^H(x, y)I_H^F(x, y) = |R||O| \exp[i\varphi(x, y)]. \quad (4)$$

Note the basic idea behind Eq. (4) is somewhat similar with the self-reference conjugate hologram method [7] in which the self-reference hologram [corresponding to $Q^H(x, y)$ in Eq. (4)] is extracted via low-pass filtering the hologram spectrum. Obviously, the linear filtering cannot distinguish the object frequency from the aberration because of the overlapping between their frequency bands, while our method does not suffer from this problem. The implicit eigen-filtering nature of identifying the dominant singular vectors provides the unwrapping and fitting with more “reliable” and less “noisy” data. Furthermore, because the unwrapping and fitting needs to be done only in one dimension, it is inherently much less complicated than the two-dimensional case. To further reduce the computational complexity, the proposed algorithm is performed only within the cropped $m \times n$ region of the whole $M \times N$ spectrum. This operation helps to avoid the highly redundant computation burden without affecting the accuracy because once the hologram is spatially filtered, the complex field is oversampled. The whole processing steps of our PCA methodology is illustrated on the right column of Fig. 1, just after the spectrum centering step. All processing is limited to the reduced $m \times n$ dimension within the spatial filter.

Experiments on human macrophage cells were performed. Figure 2(a) shows the recorded digital hologram with enlarged area showing part of the carrier fringe pattern. Figure 2(b) is the Fourier spectrum of this hologram. The maximum of the +1 order was identified, and a 160×120 rectangular filter window with the spectral maximum as center was applied. The spectrum of the hologram after spectrum centering is shown in Fig. 2(c). From the magnified three-dimensional distributions of the selected +1 order spectrum, we can see the remaining spherical wavefront broadened the spectrum to a rectangular shape so that the real center of the spectrum was fail to detect correctly. The reconstructed phase, Fig. 2(d), shows concentric circular patterns introduced

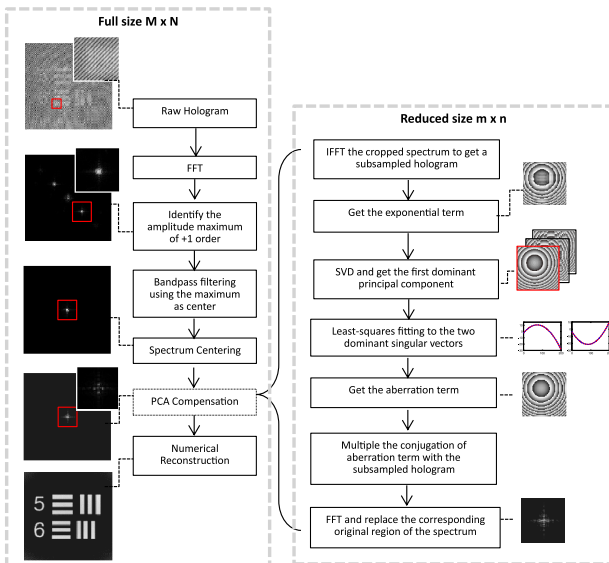


Fig. 1. Block diagram illustrating the steps involved for traditional digital holographic demodulation and reconstruction (left column) and the proposed PCA compensation algorithm (right column). Exemplary images are given for an experimental result at the output of each step.

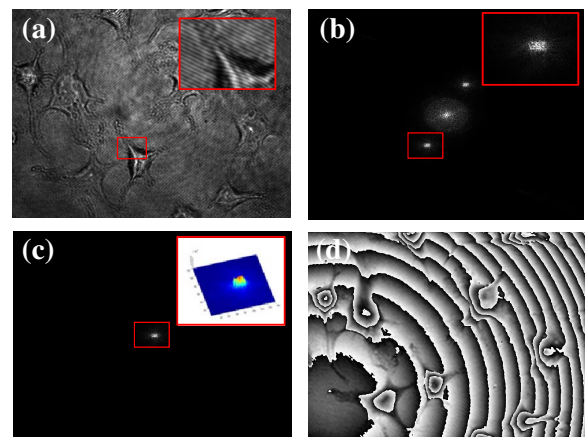


Fig. 2. Experimental results on human macrophage cells without phase aberration compensation. (a) Captured digital hologram. (b) Fourier spectrum with the red rectangle as the bandpass filter. (c) Fourier spectrum after spectrum centering. (d) Reconstructed phase map.

by the quadratic phase factor. Besides, the center of these concentric circles is shifted due to the residual tilt caused by improper spectrum centering.

We have applied the proposed algorithm to the same digital hologram and Fig. 3 shows various stages in its implementation. The cropped region with dimension 160×120 was extracted and the exponential term was analyzed by PCA. Figure 3(a) shows the reconstructed phase by rank one approximation from the first dominant singular vectors. Perhaps surprisingly, almost all phase aberration terms were separated from the objects phase if we compare Fig. 3(a) with Fig. 2(d). The singular value for this dominant phase component is about 3.5 times larger than that of second dominant one, validating the one principal component approximation. If we further add the second and third dominant components, the object phase information gradually appears, as shown in Figs. 3(b) and 3(c), respectively. The phase of the two dominant singular vectors was then unwrapped and fitted by least-squares parabolic functions [Figs. 3(d) and 3(e)]. The final estimated phase aberration term $Q(x, y)$ is shown in Fig. 3(f), demonstrating improvement in smoothness compared with the raw phase by rank one approximation [Fig. 3(a)]. By multiplying Q^{H^*} with the subsampled hologram and replacing the original region in the full size spectrum with the modified one, the

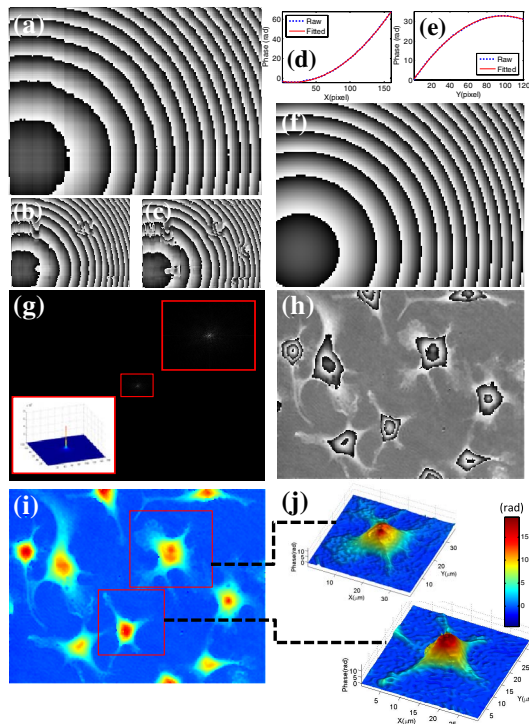


Fig. 3. Phase aberration compensation using the proposed PCA algorithm. (a) The rank one phase aberration approximation formed from the dominant singular vectors. (b) and (c) show the phase reconstructed from the first two and three sets of the dominant singular vectors, respectively. (d) and (e) The unwrapped left and right dominant singular vectors and their corresponding quadratic fitted ones. (f) The obtained phase aberration map. (g) Fourier spectrum after aberration compensation. (h) Reconstructed phase map. (i) Unwrapped phase map. (j) Pseudo-three-dimensional plot of two individual cells indicated by red boxes in (i).

spectrum of compensated hologram was obtained, as shown in Fig. 3(g). The compensated spectrum shows a concentrated distribution with a sharp peak located at the center of both the rectangular box and the whole spectrum. Using the angular spectrum algorithm for reconstruction, the wrapped phase image free from phase aberration was obtained, as shown in Fig. 3(h). Figure 3(i) shows the color-coded unwrapped phase distribution and Fig. 3(j) highlights the three-dimensional rendering of two individual cells. Subcellular features as well as the thin borders of the cells can be clearly observed without any curved or tilted background perceivable. The whole processing time is only 0.091 s, using a 2.67 GHz laptop and processing with MATLAB, which is approximately one order of magnitude faster than the least-squares surface fitting method reported in [9]. Besides, not just limited to tilt and defocus, our method can be extended to correct some high-order phase aberrations provided that only non-cross terms exists [8].

In conclusion, we have proposed a novel method to automatically compensate phase aberrations in DHM based on PCA. The advantages of the method are three-fold. First, phase aberration can be directly extracted without any manual operation or preknowledge of the setup. Second, by separating the aberration terms to two singular vectors, phase unwrapping and fitting of the data is reduced to one dimension. Finally, implementation in cropped spectrum without redundant data enables a very fast processing speed. Quantitative phase reconstruction of biological samples demonstrates the capability and good performance of the proposed method, rendering it a promising new technique for applications where the processing time is restrictive.

This project was supported by the Research Fund for the Doctoral Program of Ministry of Education of China (No. 20123219110016). C. Zuo gratefully acknowledges the financial support from China Scholarship Council (No. 201206840009).

References

1. E. Cuche, P. Marquet, and C. Depeursinge, *Appl. Opt.* **38**, 6994 (1999).
2. W. Zhou, Y. Yu, and A. Asundi, *Opt. Laser Eng.* **47**, 264 (2009).
3. C. Mann, L. Yu, C.-M. Lo, and M. Kim, *Opt. Express* **13**, 8693 (2005).
4. W. Qu, C. O. Choo, V. R. Singh, Y. Yingjie, and A. Asundi, *J. Opt. Soc. Am. A* **26**, 2005 (2009).
5. Q. Weijuan, Y. Yingjie, C. O. Choo, and A. Asundi, *Opt. Lett.* **34**, 1276 (2009).
6. T. Colomb, E. Cuche, F. Charrière, J. Kühn, N. Aspert, F. Montfort, P. Marquet, and C. Depeursinge, *Appl. Opt.* **45**, 851 (2006).
7. T. Colomb, J. Kühn, F. Charrière, C. Depeursinge, P. Marquet, and N. Aspert, *Opt. Express* **14**, 4300 (2006).
8. T. Colomb, F. Montfort, J. Kühn, N. Aspert, E. Cuche, A. Marian, F. Charrière, S. Bourquin, P. Marquet, and C. Depeursinge, *J. Opt. Soc. Am. A* **23**, 3177 (2006).
9. J. Di, J. Zhao, W. Sun, H. Jiang, and X. Yan, *Opt. Commun.* **282**, 3873 (2009).
10. P. Ferraro, S. De Nicola, A. Finizio, G. Coppola, S. Grilli, C. Magro, and G. Pierattini, *Appl. Opt.* **42**, 1938 (2003).
11. L. Miccio, S. Grilli, P. Ferraro, A. Finizio, L. De Petrocellis, and S. D. Nicola, *Appl. Phys. Lett.* **90**, 041104 (2007).